THE JOURNAL OF PHYSICAL CHEMISTRY B

Article

pubs.acs.org/JPCB

Comparative Photoactivity and Stability of Isolated Cyanobacterial Monomeric and Trimeric Photosystem I

David R. Baker,[†] Amy K. Manocchi,[†] Melissa L. Lamicq,[‡] Meng Li,[‡,§] Khoa Nguyen,[‡] James J. Sumner,[†] Barry D. Bruce,[‡,§,∥] and Cynthia A. Lundgren*[,†]

[†]Sensors and Electron Devices Directorate, United States Army Research Laboratory, Adelphi, Maryland 20783, United States

[‡]Biochemistry and Cellular and Molecular Biology Department, [§]Energy Science and Engineering Program, Bredesen Center for Interdisciplinary Research and Education, and [∥]Chemical and Biomolecular Engineering Department, University of Tennessee, Knoxville, Tennessee 37996, United States

Supporting Information

ABSTRACT: Photoactivity of native trimeric, and non-native monomeric Photosystem I (PSI) extracted from *Thermosynechococcus elongatus* is compared in a photoelectrochemical system. The PSI monomer is isolated by disassembling a purified PSI trimer using a freeze−thaw technique in presence of the short-chain surfactant, octylthioglucoside. Photoactive electrodes are constructed with PSI, functioning as both light absorber and charge-separator, embedded within a conductive polymer film. Despite structural differences between PSI trimers and monomers, electrodes cast with equal chlorophyll-a concentration generate similar photoactivities. Photoaction spectra show that all photocurrent derived from electrodes of PSI and conductive polymer originates solely from PSI with no photocurrent caused by redox mediators in the conductive polymer film. Longevity studies show that the two forms of PSI photodegrade at the same rate while exposed to equal intensities of 676 nm light. Direct photo-oxidation measurements indicate that PSI's monomeric form has fewer light harvesting antennae than trimer, and also shows energy sharing between monomeric subunits in the trimer. The structure of PSI is also found to impact cell performance when applying light at incident powers above 1.5 mW/cm^2 due to the reduced optical cross-section in the monomer, causing saturation at lower light intensities than the trimer.

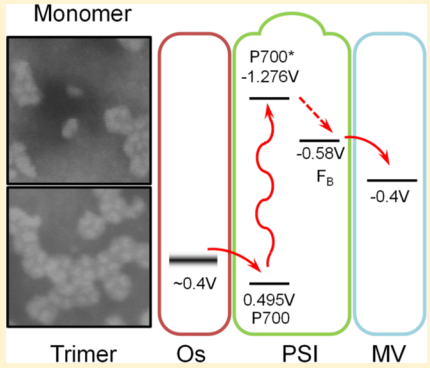

INTRODUCTION

Photosystem I (PSI) is a key protein in photosynthesis that has recently demonstrated its value as a light harvester in photovoltaic and solar fuel applications.[1−8] In nature, PSI generates reductive electrons for efficient energy storage up to 8% quantum yield for CO_2 uptake per absorbed photon.[9] Light energy absorbed by the ∼100 chlorophyll molecules within PSI is rapidly funneled to a chlorophyll dimer reaction center, P700, where charge separation occurs and an electron is passed to PSI's electron transfer chain, leaving a photogenerated hole on P700. This process operates with an internal quantum efficiency near unity, where the resulting excited electrons exist with lifetimes on the millisecond time scale at a potential of −0.58 V versus NHE.[10,11] PSI's ability to be an efficient generator of long-lived, reductive electrons that are accessible to soluble electron scavengers, has made it the preferred reaction center for biohybrid solar energy harvesting studies.

Two oligomeric forms of PSI are found in nature: a monomeric form most commonly found in plants and algae and a trimeric form found in blue green algae, with the most well-characterized trimer originating from the thermophilic cyanobacteria, *Thermosynechococcus elongatus* (*T.e.*).[12] The PSI trimer in *T.e.* is composed of three monomers that associate to form a disc-shaped protein complex, approximately 22 nm in diameter and 9 nm in height. This trimer complex enables a small amount of energy transfer to occur between the adjacent PSI monomers, which has been shown to be beneficial in low light environments (monomeric plant PSI has alternatively evolved to associate with LHC-I for low light situations).[13,14]

When constructing photoelectrochemical devices, research groups have interchangeably used either monomeric (from plants) or trimeric (from cyanobacteria) forms of PSI.[6,8,15] The activity of the various PSI systems is commonly compared based on the concentration of chlorophyll-a. This method equates the monomer and trimer with respect to absorption capacity but disregards any potential structural effects of the different proteins. For example, the aspect ratio, surface area, and protein surface characteristics differ significantly between monomeric and trimeric forms of PSI. These differences affect surface assembly, device design, and association with interacting proteins or mediators.[4,12] Also, the two oligomeric states across various species possess different ratios of chlorophyll-a molecules to reaction centers.[12,16] In addition to structural differences, the two types of PSI use different charge transfer

Received: August 8, 2013
Revised: February 18, 2014
Published: February 18, 2014

proteins to extract photogenerated holes from the positive origin of the central electron transfer pathway (P700 site).[17,18] The resulting charge transfer kinetics are strikingly different.[18,19] Any comparison between the two quaternary structures of PSI should therefore involve a monomer that is derived from the mature trimer and not an early assembly intermediate that may lack cofactors and subunits. If the oligomeric form of PSI is indeed insignificant to the photoelectrochemical performance, there could be a great advantage to making electrode assemblies with the monomer over the native trimer, such as denser surface packing or alternative electrode binding sites. Therefore, a direct photoelectric activity comparison needs to be made between monomeric and trimeric forms of PSI.

This paper compares the native *T.e.* PSI trimer to a *T.e.* PSI monomer that has been derived from disassembling a native *T.e.*'s trimer complex. To photoelectrochemically compare the two structures, PSI monomer or trimer was embedded within a conductive redox polymer film, based on work by Rögner et al. where a conductive polymer system was developed to entrap PSI.[20,21] The redox polymer film is able to extract photogenerated holes from the P700 site using the redox mediator osmium bis 2,2′-bipyridine chloride ($Os(bpy)_2Cl_2$). $Os(bpy)_2Cl_2$ is able to pass electrons through the polymer film by diffusion if it is unbound and by a hopping mechanism if attached to the polyvinylimidazole (PVI) polymer backbone.[22,23] Excess unbound $Os(bpy)_2Cl_2$ is capable of extracting photogenerated holes from the excited P700 site, then transferring them to polymer bound $Os(bpy)_2Cl_2$, or it can diffuse through the polymer film and donate holes directly to the backing electrode. The PVI film is also porous enough to allow water and other redox mediators to diffuse into the film and scavenge photoelectrons from the Fe−S acceptors on the stromal surface of PSI. By using a polymer matrix to encapsulate PSI, orientation limitations are mitigated, which otherwise would hamper electrodes made from PSI monolayers, due to the steric differences between monomeric and trimeric PSI as well as the larger dipole moment of the trimer. Because of the three-dimensional structure and high loading densities of PSI, this redox-polymer configuration was able to produce electron turnover rates similar to demonstrations of PSI in suspension with cytochrome c_6 (cyt c_6) and ascorbic acid.[8,24] This rapid electron turnover rate enabled this study to investigate the differences between monomeric and trimeric PSI configurations in $Os(bpy)_2Cl_2$/PVI films.

EXPERIMENTAL SECTION

PSI Purification. PSI was isolated from the thylakoid membranes of the thermophilic cyanobacteria *T.e.*, as described previously.[6] Briefly, *T.e.* cells were exposed to lysozyme for 45 min at 37 °C, then lysed via three passes through a French press cell disrupter (Thermo Scientific) at 20000 psi. Thylakoid membranes were then collected by centrifugation at 45000*g*. The membranes were washed three times, including a wash with 1.5 M NaBr and solubilized with incubation in 0.2% (w/v) *N*-dodecyl *β*-D-maltoside (DDM) (Glycon Biochemicals, Luckenwalde, Germany). Soluble proteins were separated from membranes via centrifugation at 45000*g* and then loaded onto a 10−30% linear sucrose gradient (20 mM MES pH 6.4, 10 mM $CaCl_2$, 10 mM $MgCl_2$, and 0.03% w/v DDM) for 16 h at 24000 rpm using a SW 32-Ti Rotor. The lower green band, containing intact PSI trimers, was collected and then purified using anion exchange chromatography via HPLC. PSI was stored at a final concentration of 4.73 mg/mL PSI in 20 mM MES pH 6.4, 10 mM $CaCl_2$, 10 mM $MgCl_2$, and 0.03% w/v DDM.

PSI Monomerization. PSI trimer from *T.e.* was diluted to have a 1 mg/mL chlorophyll-a concentration. The detergent octylthioglucoside (OTG) was added at a concentration of 0.375% w/v to the trimeric PSI. The PSI and detergent mixture was placed in a 55 °C water bath for 5 min then cooled in an ice/water bath for 2.5 min. This cycle was repeated 18 times. The treatment allowed for a lipid-phase transition to occur which, when coupled with the micelle formed by the detergent, encouraged the dissociation of native PSI. Following the treatment, a stepwise sucrose gradient was made for the isolation of the monomeric PSI, and run at 28000 rpm for 16 h using a SW 32-Ti rotor. Two resulting bands from centrifugation were representative of the trimeric and monomeric state, the latter being the upper band in the gradient. The monomeric band was then extracted. A native-PAGE Bis-Tris gel 4−16% was then run to identify the monomerized PSI in comparison to the trimeric complex.

PVI and $Os(bpy)_2Cl_2$ Preparation. The backbone polymer polyvinylimidazole (PVI) was prepared by mixing 0.2 mL of allylamine with 3 mL of vinylimidazole and 240 mg 2,2′-azobis(isobutyronitrile) in an argon atmosphere. The mixture was heated to reflux for 2 h. After cooling to room temperature, 6 mL of ethanol was used to dissolve the polymer. This solution was added dropwise into 60 mL of acetone under heavy stirring. The precipitate was filtered and washed with 10 mL of acetone. The resulting filtrate was dried at 50 °C overnight under vacuum.[21]

The osmium redox complex osmium bis 2,2′-bipyridine chloride ($Os(bpy)_2Cl_2$) was prepared by mixing 0.34 g 2,2′-bipyridyl, 0.5 g K_2OsCl_6, and 20 mL of dimethylformamide (DMF) in a 100 mL round-bottom flask and refluxed for 1 h. Solid KCl was removed by filtration, and 250 mL of diethyl ether was added dropwise to the remaining liquid solution, while stirring. Once mixed, the solution was stirred for an additional 1 h. The resulting precipitate was filtered, dried, and resuspended in a mixture of 10 mL of DMF and 5 mL of methanol. A total of 100 mL of an aqueous solution containing 1 g $Na_2S_2O_4$ was slowly added to the osmium solution, while stirring. To induce crystallization, the flask was placed in an ice bath. The precipitate was then filtered, washed with water and ethanol, and then dried.[25]

To incorporate $Os(bpy)_2Cl_2$ into the polymer, 210 mg PVI and 150 mg $Os(bpy)_2Cl_2$ were mixed in 95 mL of ethanol, and refluxed while stirring for three days. The solution was precipitated by adding diethylether and filtered. The filtrate was resuspended in ethanol and then dried. The resulting redox polymer (PVI/Os) was suspended in water at 10 mg/mL for storage and use in experiments.

PSI Characterization. P700 photo-oxidation was tested using pump−probe transient absorption spectroscopy with a BioLogic Joliet-type spectrometer, JTS-10. Photobleaching of P700 was measured at 705 nm by varying both the incident photon flux, and the illumination time. The UV−vis absorbance spectra of PSI in 20 mM MES buffer was obtained using a Jasco J-815 CD-Spectrophotometer (Jasco Analytical Instruments, Easton, MD). Scanning transmission electron microscope (STEM) images were obtained using a Ziess Auriga at 30 kV after staining the protein with 1% uranyl acetate.

Electrode Fabrication. Electrodes (0.8 × 2.5 cm) were cut from ITO-coated glass slides (15−25 Ω, Cytodiagnostics,

Scheme 1. Assembly Process of the PVI/Os/PSI Film[a]

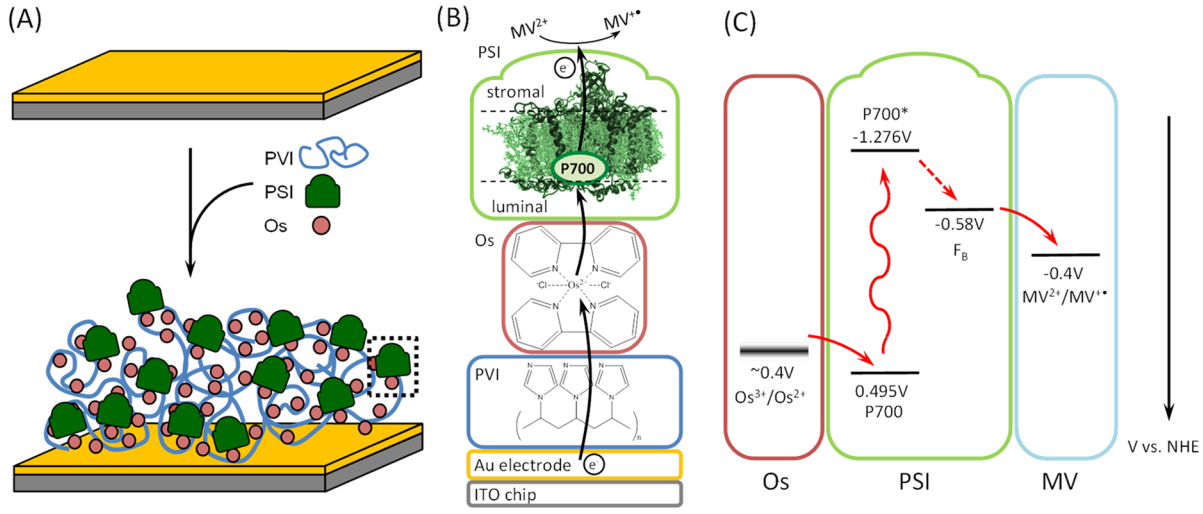

[a](A) Constituents are mixed and then dropcast onto a Au-coated ITO electrode. The dried film consists of randomly oriented proteins. The cathodic electron transfer pathway (B) consists of electrons transferred from the Au electrode to $Os(bpy)_2Cl_2$ redox centers, then to PSI, and finally scavenged by MV^{2+} at the stromal side of PSI. The energy level diagram (C) shows the electron pathway from $Os(bpy)_2Cl_2$ through PSI to MV^{2+} with PSI energy level potentials vs NHE reported from literature[10] and redox mediator potentials determined by cyclic voltammetry.

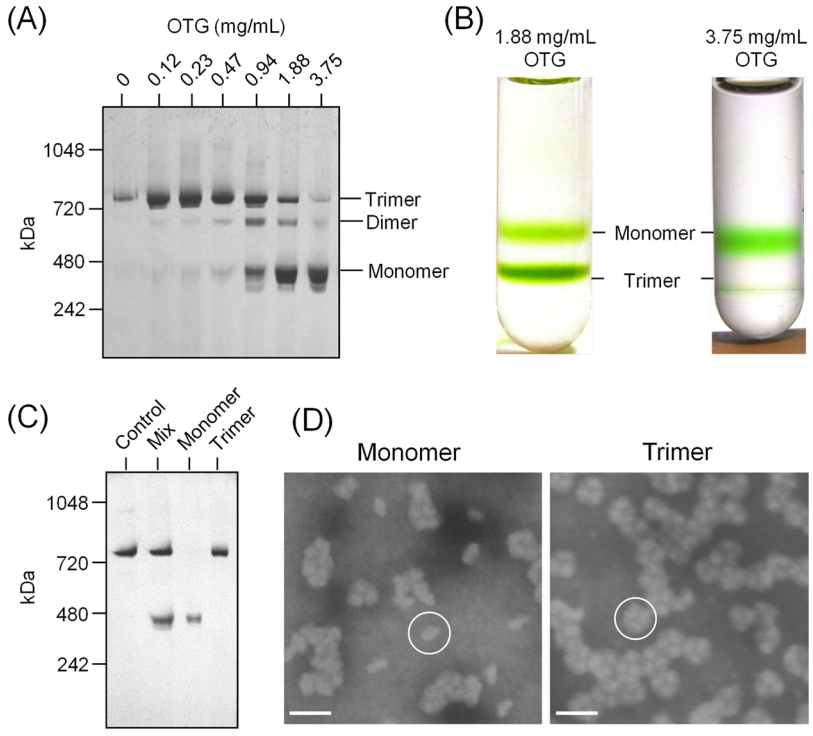

Figure 1. PSI monomer preparation from PSI trimer. (A) BN-PAGE of freeze−thaw treated PSI trimer with different concentration of detergent octylthioglucoside (OTG). (B) Separation of PSI trimer from monomer using sucrose density gradient ultracentrifugation demonstrating the different yields using 1.88 and 3.75 mg/mL OTG. (C) BN-PAGE of isolated PSI monomer and trimer. Control and mix represents untreated and treated PSI trimer using 1.88 mg/mL OTG. Monomer and trimer bands are after separation of the mixture with OTG. (D) STEM images of PSI monomer and trimer. Scale bar is 30 nm, with examples of individual monomers and trimers circled.

Burlington, ON) and coated with 200 nm of Au, over a 10 nm Ti adhesion layer deposited by e-beam evaporation. As depicted in Scheme 1, to create active films a mixture of 10 μL PVI/Os (10 mg/mL), 2.3 μL of poly(ethylene glycol) (N) diglycidyl ether (PEGDGE, 5 mg/mL), and 6.7 μL of PSI was dropcast onto a 1 cm^2 area on the Au chip. The films were air-dried overnight in the dark, then soaked in 250 μM methyl viologen dichloride (MV^{2+}) and 0.1 M $MgCl_2$ for 5 min, and finally rinsed with DI-H_2O prior to use.

Electrode Characterization. Photoelectrochemical measurements were conducted using a Reference 600 potentiostat (Gamry Instruments, Warminster, PA) in a three electrode configuration with an Ag/AgCl (3 M KCl) reference electrode, and Pt wire counter electrode in a quartz cell. The electrolyte was an aqueous solution consisting of 250 μM MV^{2+}, 32 μM

dx.doi.org/10.1021/jp407948p | J. Phys. Chem. B 2014, 118, 2703−2711

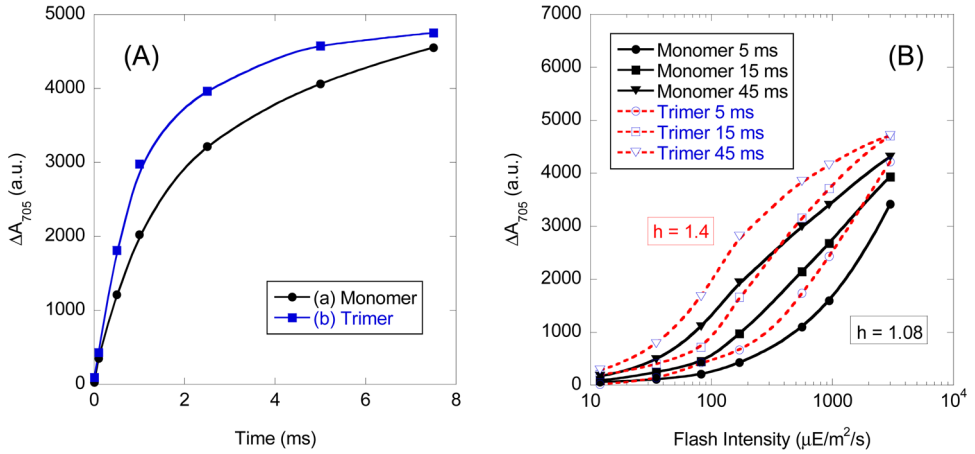

Figure 2. Transient absorption of monomer and trimer PSI with various flash times (A) and different flash intensities (B). The monomer and trimer were fit to determine the Hill coefficients.

$Os(bpy)_2Cl_2$, and 0.1 M $MgCl_2$. Incident light was produced by a 130 W Xe lamp (Newport Corporation, Irvine, CA) and filtered by a 676 nm band-pass filter. Unless otherwise indicated, the applied potential in the cell was −0.2 V versus Ag/AgCl. All photocurrent tests were conducted at an incident power of 1.4 mW/cm^2 unless otherwise specified.

RESULTS AND DISCUSSION

The PSI monomer from *T.e.* was isolated from native PSI trimers via a freeze−thaw treatment in the presence of the surfactant octylthioglucoside (OTG), as described in the Experimental Section. This freeze−thaw treatment caused the trimer complex to dissociate into its individual monomers, whereby the newly exposed hydrophobic surfaces of the protein were passivated by OTG to prevent reassociation. Figure 1A depicts how the concentration of OTG in the freeze−thaw process dictates the monomeric yield. At a concentration of 3.75 mg/mL OTG, the resulting PSI is nearly all monomer, with only a trace of trimer left, as also evidenced by band coloration in the sucrose gradient (Figure 1B). After purifying by extracting bands from the sucrose gradient a BN-PAGE (Figure 1C) showed that the isolated PSI was pure of other oligomeric states. A dimer was observed to also form during the treatment, especially in intermediate OTG concentrations, but was dissociated into monomers at 3.75 mg/mL OTG. Figure 1D shows STEM images of dispersed purified PSI monomer and trimer. It is seen that circular trimeric oligomers are lost once the monomerization process is completed. The resulting monomeric units were oblong in shape, with a narrow width of ∼10 nm and a length of ∼16 nm; whereas the trimer groups were circular in shape with a diameter of ∼22 nm.

Prior work has shown that exciton energy can be transferred between adjacent monomeric subunits of cyanobacterial PSI trimeric complexes.[6] In addition to increasing the optical cross-section, for benefit in low-light environments, it has also been proposed to help allow excess energy dissipation to protect against photo destruction under high light conditions.[14] This pathway permits absorbed photon energy to be quickly transferred to one of the two adjacent monomers through chlorophyll antenna molecules if the initial P700 is already in a photoexcited state. This energy may then be successfully utilized upon transfer for photochemical processes.

Using transient absorption spectroscopy it was seen that energy transfer between joined monomeric subunits does lead to more efficient photo-oxidation in the trimer versus the monomer. As shown in Figure 2A, the optical signature of P700 photo-oxidation (ΔA_{705}) is greater for the trimer than the monomer at short flash durations, with equal chlorophyll-a concentrations. To control for contributions of light history, a fresh sample was used for each illumination measurement. The absorbance change for each flash time was read three times and the average was graphed. Although three separate P700 photobleaching measurements were made for each flash time, the variation between reads was very small and much less that the size of the graphing symbol. As the flash duration approaches >8 ms, the samples become light saturated, and the photobleaching signal converges to a common value. This indicates a mechanism with native trimers, in which energy transfer may occur between monomers, where energy from chlorophyll-a of an oxidized monomer may travel to an adjacent reduced monomer in order to oxidize it.

When ΔA_{705} was plotted against the log value of the incident photon flux (Figure 2B), a sigmoidal relationship arises. A fit to one site-specific binding was calculated relating to the cooperation between the adjacent monomers. This analysis uses a fit from all three exposure times (5, 10, and 15 ms) for both the monomer and the trimer. This experiment allows direct comparison of the effective optical cross-section of the two different oligomeric forms of PSI. This calculation was similar to what was observed between cooperative allosteric enzymes, and can be reported as a Hill coefficient.[26] The monomer's Hill coefficient is near 1 (1.08 ± 0.044) indicated very little energy transfer or antenna coupling in monomeric PSI. However, the native trimeric form of PSI displays significant coopertivity (h = 1.4 ± 0.097). This implies that under continuous illumination individual P700 sites turned over markedly more in the trimer than in the monomer.

Comparisons between the photoactivity of monomeric and trimeric forms of PSI were conducted by interpreting photocurrent obtained from PSI entrapped in the conductive polymer PVI/Os. Aliquots of PSI monomer and trimer stock were mixed with PVI/Os redox polymer solutions and dried on Au/ITO electrodes, as shown in Scheme 1A. The amount of PSI in the monomer and trimer samples was controlled by chlorophyll-a concentration to maintain equal light absorbance for each electrode. The samples were then soaked in a solution similar to the photoelectrochemical electrolyte (250 μM MV^{2+}, 0.1 M $MgCl_2$, $Os(bpy)_2Cl_2$) to extract excess unbound

dx.doi.org/10.1021/jp407948p | J. Phys. Chem. B 2014, 118, 2703−2711

$Os(bpy)_2Cl_2$ by diffusion from the polymer films and bring the electrodes close to equilibrium with the photoelectrochemical test cell. This process limited transient background currents and maintained a known concentration of mediator species in the polymer film. The photoelectrochemical electrolyte solution contained two mediators to extract charges from PSI, 250 μM MV^{2+} to extract excited electrons from iron−sulfur centers on the stromal side of PSI, and 32 μM $Os(bpy)_2Cl_2$ to collect photogenerated holes from the P700 site on the luminal side.

During photocurrent measurements, electrodes were exposed to incident light (676 nm band-pass filtered) and placed under a potential bias (−0.2 V vs Ag/AgCl). The monomer and trimer samples produced cathodic photocurrents similar to each other, as shown in Figure 3a and b, respectively, where

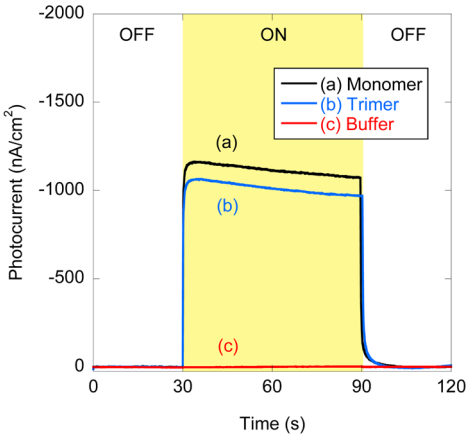

Figure 3. Photocurrent of electrodes under 1.4 mW/cm^2, 676 nm light, and −0.2 V vs Ag/AgCl potential bias. Electrodes were made with 0.1 mg Chl/mL stock solutions of monomeric (a) and trimeric (b) PSI. The blank sample (c) used an equal volume of storage buffer in place of PSI.

background currents were subtracted for clarity. Cathodic currents are designated in this study as negative currents. Figure 3 shows typical results where the two forms differ by approximately 10%. Variability caused by heterogeneity in the dropcast films caused photocurrents to span a range of values. Within this variability there was no observable difference between photocurrent from monomer films or trimer.

For comparison, a blank sample (Figure 3c), consisting of a PVI/Os electrode with supporting buffer in place of PSI, was also tested as a control. No change in current of the blank sample was observed when the light was turned on or off. Importantly, there was no observable signal from $Os(bpy)_2Cl_2$ redox centers in either the polymer film or electrolyte solution which absorb light in the green and blue regions of the visible spectrum. Therefore, it was clear that PSI was necessary for producing photocurrent.

Free $Os(bpy)_2Cl_2$ in the electrolyte solution was also found essential to reasonably access PSI electrochemically in the polymer matrix. In experiments without free $Os(bpy)_2Cl_2$ in the electrolyte solution the only source of $Os(bpy)_2Cl_2$ to interact with PSI was in the polymer film, and could exist as either bound to the polymer film or as a free unbound, able to diffuse out of the film. If an electrode was not presoaked to remove excess unbound $Os(bpy)_2Cl_2$ before testing, as described above, the resulting photocurrent was found to be extremely dynamic. The photocurrent from these unsoaked electrodes increased initially as the polymer absorbed electron scavenging mediators (MV^{2+}), and then decayed as unbound $Os(bpy)_2Cl_2$ diffused out of the film, Figure S1. This demonstrates that the concentration of loose $Os(bpy)_2Cl_2$ in the polymer film greatly impacted the stability of photoactivity and the need for pre-equilibrating electrodes.

Photogenerated holes lay at P700 which is coordinated by the protein subunits PsaA/B and is 1.6 nm from the luminal surface. In vivo, these holes are reduced via specific docking and electron transfer from the metalloprotein cyt c_6.[12] The presence of $Os(bpy)_2Cl_2$ in the electrolyte solution allowed for faster diffusion to and away from the P700 site than was possible for the $Os(bpy)_2Cl_2$ centers bound to the polymer backbone. This increased mobility supported much higher photocurrents than observed with only the mediators bound to the polymer. The presence of redox centers bound to the polymer may not be required for this particular system to function, but if a true solid state system is to be developed it would be; though investigations into this area are beyond the scope of this paper. It should also be noted that several studies have demonstrated the ability to extract charges from the P700 site without redox mediators, but only with native monomer isolated from plants.[7,15,27] Structural differences between plant and *T.e.* protein subunits on the luminal surface, specifically subunit PsaF, may be a reason *T.e.* required a mobile charge

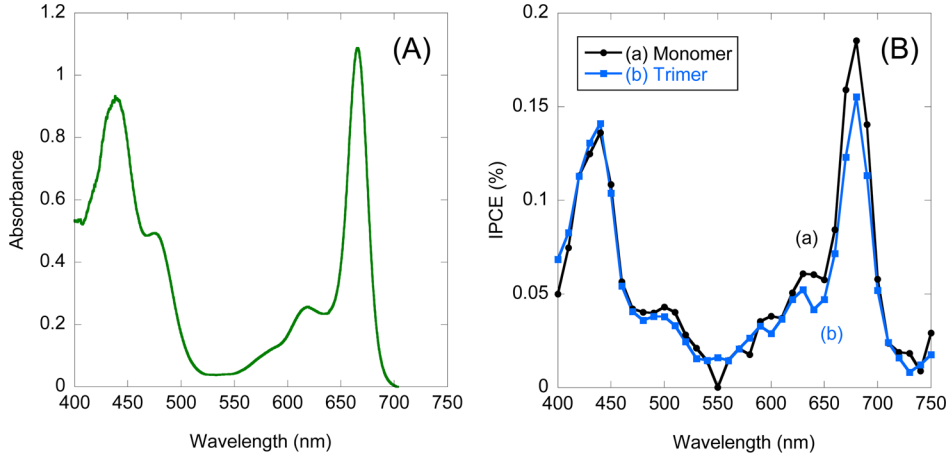

Figure 4. Absorbance spectrum (A) of PSI trimer solution. IPCE photoaction spectra (B) of PSI monomer (a) and trimer (b).

dx.doi.org/10.1021/jp407948p | J. Phys. Chem. B 2014, 118, 2703−2711

extractor. These differences in charge extraction exemplify the need to use a single species when comparing monomeric and trimeric PSI.

The control test of a PVI/Os electrode with no PSI, shown in Figure 3c, implied that PSI was the origin of photocurrent in the present system. However, there are other factors that could cause photocurrent to appear when PSI was added, such as contaminants in the PSI stock photodegrading or interacting with the $Os(bpy)_2Cl_2$. Therefore, to explicitly confirm that all photocurrent was generated solely from PSI the photoaction spectra for monomer and trimer samples were obtained, as shown in Figure 4. The incident photon to charge carrier efficiency (IPCE) is an external quantum efficiency measurement that measures an electrode's activity as a function of wavelength and is related through eq 1.

$$\mathrm{IPCE}(\%) = \frac{1240 \cdot \mathrm{I(A/cm^2)}}{\lambda(\mathrm{nm}) \cdot \mathrm{P(W/cm^2)}} \times 100\% \quad (1)$$

An IPCE spectrum should match the absorbance spectrum of the desired light absorber without any additional signal which would indicate photodegradation or contribution from impurities. As seen in Figure 4, the IPCE spectrum closely follows the absorbance spectrum of PSI, demonstrating that PSI is the only source of photoelectrons. Most importantly, the IPCE spectrum shows no signal onset at 550 nm as would be expected if $Os(bpy)_2Cl_2$ was a contributing species, due to its absorbance in the green and blue regions of the visible spectrum (Figure S2). Also, there is no noticeable background signal, indicating that photocurrent does not contain measurable electrons scavenged from photodegradation reactions. The IPCE results, therefore, confirmed the observations made in Figure 3c; that PSI was the sole source of photocurrent. Additionally, the explicit values of IPCE spectrum for the two forms of PSI were similar, indicating that structure had no apparent impact on the spectral properties or activity of PSI. This observation is not surprising since the two forms of PSI use the same light absorbing molecules at the same concentration for the electrodes tested.

In Figure 5, the concentrations of both PSI monomer and trimer used in electrode fabrication were varied in order to determine the effect of PSI loading on photocurrent. In the surface concentration range of 0.5 to 3 mg/mL PSI, for both monomer and trimer, photocurrent was found to be linearly proportional to PSI surface concentration. A large variability caused by inherent heterogeneities in the dropcasting process likely caused the widespread in observed values. The structure of PSI did not exhibit any favorability to produce higher photocurrent for one oligomeric state above the film variability.

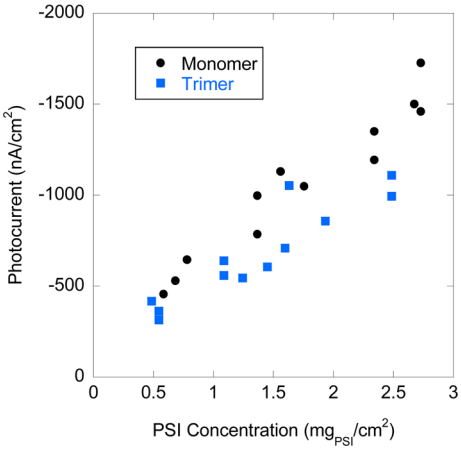

Figure 5. Photocurrent vs PSI surface concentration for both monomer (black circles) and trimer (blue squares).

Because the PSI monomer was in a non-native state and was presumably more susceptible to photodegradation, an extended illumination study was performed to observe how electrodes of both PSI forms retain photocurrent under extended periods of illumination. As seen in the longevity plot of Figure 6, PSI

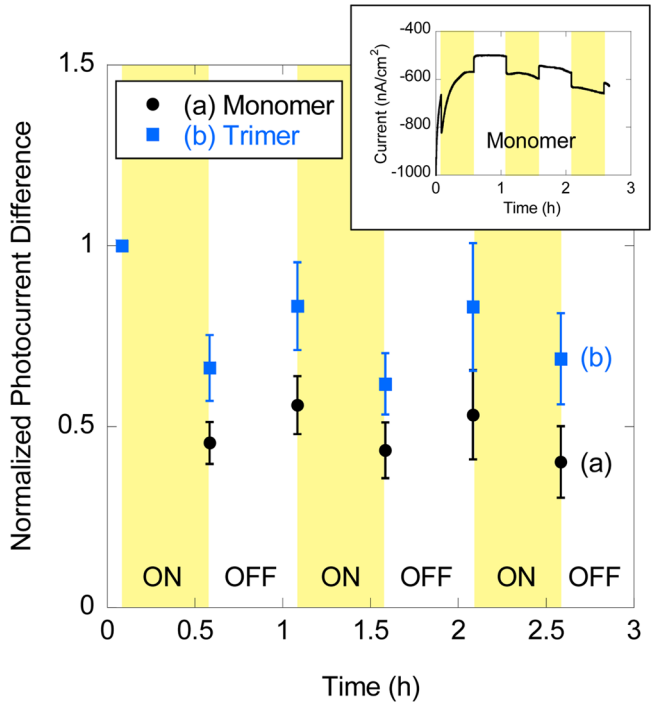

Figure 6. Longevity test of monomer (a) and trimer (b) electrodes constructed with a surface concentration of 2.5 mg PSI/cm^2, measuring the current step difference when the light is turned on or off in 30 min cycles. Photocurrent was normalized to the initial photocurrent of each cell. Error bars are 95% confidence intervals. Inset shows a representative current−time plot depicting the changes in current when the light was switched on and off for a typical monomer sample.

electrodes were exposed to 30 min on/off illumination cycles over the course of 3 h (as opposed to the 1 min cycles in other sections of this study). The photocurrent was reported as normalized photocurrent differences in Figure 6 to compare activity on the same scale when the light was turned on and off. When the photocurrent was normalized to the initial photocurrent rise both monomer and trimer samples showed an initial drop in photocurrent which stabilized after the first cycle. Monomer and trimer samples decayed at similar rates after the initial drop. During the dark periods electrodes recover some of the photocurrent, though fail to return to original activity. The gradual loss of photocurrent may stem from chlorophyll degradation, leakage of active materials, or other means. Importantly, by decaying at similar rates the non-native state of *T.e.* PSI (monomer) did not appear to be less photostable than the native form of PSI (trimer). This indicates that either form can be used for long-term illumination studies.

Figure 7 shows how photocurrent was affected by differences in applied potential. The PVI/Os/PSI system became active

dx.doi.org/10.1021/jp407948p | J. Phys. Chem. B 2014, 118, 2703−2711

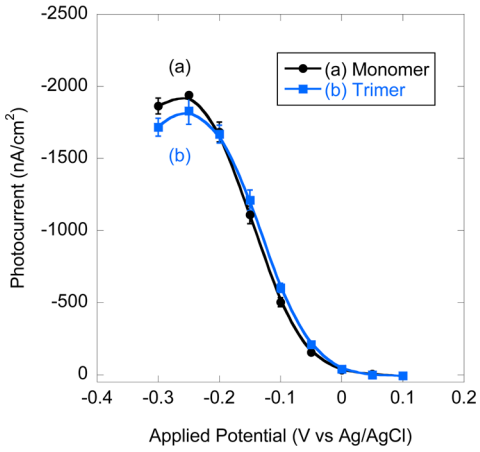

Figure 7. Applied potential vs photocurrent of monomer (a) and trimer (b) electrodes made with 0.1 mg Chl/mL PSI. Error bars are 95% confidence intervals.

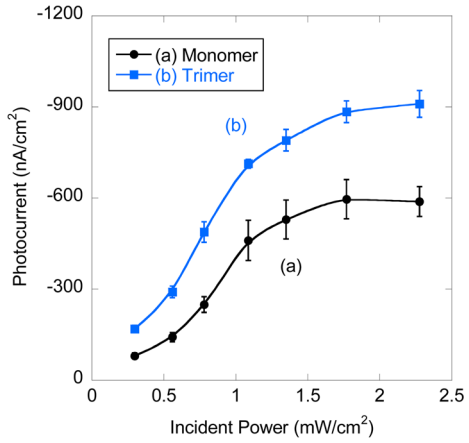

Figure 8. Photocurrent response of monomer (a) and trimer (b) electrodes at various incident light powers, wavelength 676 nm.

once a sufficiently reductive potential was applied. Starting from oxidizing potentials a current onset appeared at −0.05 V vs Ag/AgCl and grew to a plateau at −0.2 V versus Ag/AgCl for both the monomeric and the trimeric systems. The Au substrate of the working electrode transferred electrons to the $Os(bpy)_2Cl_2$ species in the polymer, which had a redox potential of 0.2 V versus Ag/AgCl (determined by cyclic voltammetry (CV) of aqueous $Os(bpy)_2Cl_2$). Potentials positive of the $Os(bpy)_2Cl_2$ redox potential are unable to facilitate redox turnover thereby requiring applied potentials negative of −0.05 V versus Ag/AgCl to activate the electrodes. The 250 mV difference between the CV reaction potential and the observed current onset is likely caused by the local environment of redox centers in the polymer film. Osmium-based redox centers have been found to be especially sensitive to coordinated ligands, pH, and other environmental parameters.[28] In Figure 7 both the monomer and trimer forms exhibit the same potential shift, which was expected since both originated from the same species, thereby exhibiting similar redox potentials for electron transfer from the redox-shifted $Os(bpy)_2Cl_2$ centers to the P700 site. The degree of potential shift infers that it is possible that $Os(bpy)_2Cl_2$ centers could be used to tune an electrode by modifying the local environment in the polymer film toward creating an active, unbiased, two-electrode system.

It has been suggested that *T.e.* naturally forms PSI trimer complexes to more efficiently harvest light at under dim conditions.[12] To investigate how electrodes of PSI monomer and trimer respond to various light levels the incident power was varied between 0.25 mW/cm^2 and 2.5 mW/cm^2, as shown in Figure 8. Below an incident power of 1 mW/cm^2 both systems showed an essentially linear response to an increase of light power, while also demonstrating similar photocurrents with the trimer slightly outpacing the monomer. Also, both samples showed a roll off with incident powers above 1 mW/cm^2, indicating that chlorophyll within PSI was becoming saturated. This roll off was the impetus for the choice of 1.4 mW/cm^2 (81 μE/m^2/s) in all other experiments, so as to have a nearly saturated electrode without photobleaching PSI. Interestingly, as the power was increased to intensities consistent with the AM 1.5 solar spectrum (2.28 mW/cm^2 at 676 nm)[29] the trimer electrodes produced 20−50% more photocurrent than monomer samples. The saturation of the monomer's photocurrent showed a leveling off at 2 mW/cm^2, whereas the trimer still showed a slight increase in photocurrent with intensity, indicating it was not fully saturated at that level, as opposed to the monomer.

The trimer's greater activity at high incident powers was attributed to extra chlorophyll-a molecules contained between monomers in the trimer complex, which were missing in the monomer system contributing to the trimer's greater maximum absorbing ability per PSI. The extra chlorophylls were also likely the origin of the energy transfer observed in Figure 2. To confirm that trimer contains more chlorophyll-a than monomeric PSI, the protein concentration of the monomer and trimer PSI solutions (with equal chlorophyll-a concentration) was measured using a Bradford protein assay. Monomerized PSI, with a chlorophyll-a concentration of 0.115 mg/mL Chl, was found to have a protein concentration of 0.22 mg/mL PSI, whereas the trimer (0.112 mg/mL Chl) was 0.18 mg/mL PSI, thus, yielding a ratio of 0.509 mg Chl/mg PSI for monomer and 0.639 mg Chl/mg PSI for the trimer. Therefore, trimeric PSI contained 25% more chlorophyll-a than the isolated monomers, which corresponds well with the range of 20−50% increase in photocurrent of trimer over monomeric electrodes at high incident powers shown in Figure 8. The difference in photocurrent may occur predominately at higher incident powers because the two forms were able to absorb light and produce photoelectrons with equal efficiencies at lower powers. Once saturated, the monomer became unable to absorb incident photons as efficiently as the trimer.

CONCLUSIONS

PSI from *T.e.* was found to be similarly active between the trimeric native form and the monomer isolated by disassembling the trimer into its constituent monomers. The similar photoactivity between monomer and trimer indicates that one can use either form of PSI without concern that structure will affect efficacy. For example, it may be more beneficial to use the smaller monomer for high surface density packing, whereas for orientation purposes, the anisotropy inherent in trimer may be more advantageous. The similarities of the monomer and trimer systems may not be unexpected, but it is important to confirm these similarities between PSI forms from a single species for future studies which would compare activities of PSI from plant to cyanobacteria. Energy transfer cooperation was found to occur between the monomeric constituents of the trimer complex. Despite this, the actual photocurrent obtained

dx.doi.org/10.1021/jp407948p | J. Phys. Chem. B 2014, 118, 2703−2711

was limited by the absorbance of the ensemble film: both for trimer and monomer. Importantly, it was also found through IPCE spectra, that photocurrent arises solely from PSI despite $Os(bpy)_2Cl_2$ having an absorption in the visible region. The only effect structure imposed on the activity of electrodes was found in the light intensity at which PSI saturates, where trimer was saturated at higher incident light power due to 25% more chlorophyll-a per reaction center than the monomer. By illuminating samples with incident powers below 1.5 mW/cm^2 of 676 nm light the differences in saturation of the two PSI forms can be neglected. Fair comparisons between monomer and trimer systems can only then accurately be made.

■ ASSOCIATED CONTENT

Supporting Information

Photocurrent comparison of unsoaked and presoaked electrodes and absorbance spectrum of $Os(bpy)_2Cl_2$. This material is available free of charge via the Internet at http://pubs.acs.org.

■ AUTHOR INFORMATION

Corresponding Author

*Phone: (301) 394-2541. E-mail: cynthia.a.lundgren2.civ@mail.mil.

Notes

The authors declare no competing financial interest.

■ ACKNOWLEDGMENTS

STEM imaging was graciously performed by Dr. John R. Dunlap at the University of Tennessee. Financial support from the U.S. Department of the Army and U.S. Army Materiel Command are gratefully acknowledged. Research was supported, in part, by a contractual appointment to the U.S. Army Research Laboratory Postdoctoral Fellowship Program administered by the Oak Ridge Associated Universities (D.R.B. and A.K.M.). M.L. has been partially supported as a CIRE Fellow from the Bredesen Center, BDB acknowledges support from TN-SCORE, a multidisciplinary research program sponsored by NSF-EPSCoR (EPS-1004083) and support from the Gibson Family Foundation. K.N., M.L., and B.D.B. acknowledge support from the UTK BCMB Department. K.N. was supported as an IGERT Fellow from the National Science Foundation IGERT Program (DGE-0801470).

■ REFERENCES

(1) Yacoby, I.; Pochekailov, S.; Toporik, H.; Ghirardi, M. L.; King, P. W.; Zhang, S. G. Photosynthetic Electron Partitioning Between [FeFe]-Hydrogenase and Ferredoxin: NADP(+)-Oxidoreductase (FNR) Enzymes In Vitro. *Proc. Natl. Acad. Sci. U.S.A.* **2011**, *108*, 9396−9401.

(2) Utschig, L. M.; Silver, S. C.; Mulfort, K. L.; Tiede, D. M. Nature-Driven Photochemistry for Catalytic Solar Hydrogen Production: A Photosystem I-Transition Metal Catalyst Hybrid. *J. Am. Chem. Soc.* **2011**, *133*, 16334−16337.

(3) Krassen, H.; Schwarze, A.; Friedrich, B.; Ataka, K.; Lenz, O.; Heberle, J. Photosynthetic Hydrogen Production by a Hybrid Complex of Photosystem I and [NiFe]-Hydrogenase. *ACS Nano* **2009**, *3*, 4055−4061.

(4) Manocchi, A. K.; Baker, D. R.; Pendley, S. S.; Nguyen, K.; Hurley, M. M.; Bruce, B. D.; Sumner, J. J.; Lundgren, C. A. Photocurrent Generation from Surface Assembled Photosystem I on Alkanethiol Modified Electrodes. *Langmuir* **2013**, *29*, 2412−2419.

(5) Gerster, D.; Reichert, J.; Bi, H.; Barth, J. V.; Kaniber, S. M.; Holleitner, A. W.; Visoly-Fisher, I.; Sergani, S.; Carmeli, I. Photocurrent of a Single Photosynthetic Protein. *Nat. Nanotechnol.* **2012**, *7*, 673−676.

(6) Iwuchukwu, I. J.; Vaughn, M.; Myers, N.; O'Neill, H.; Frymier, P.; Bruce, B. D. Self-Organized Photosynthetic Nanoparticle for Cell-Free Hydrogen Production. *Nat. Nanotechnol* **2010**, *5*, 73−79.

(7) Ciesielski, P. N.; Scott, A. M.; Faulkner, C. J.; Berron, B. J.; Cliffel, D. E.; Jennings, G. K. Functionalized Nanoporous Gold Leaf Electrode Films for the Immobilization of Photosystem I. *ACS Nano* **2008**, *2*, 2465−2472.

(8) Lubner, C. E.; Grimme, R.; Bryant, D. A.; Golbeck, J. H. Wiring Photosystem I for Direct Solar Hydrogen Production. *Biochemistry* **2009**, *49*, 404−414.

(9) Ehleringer, J.; Bjorkman, O. Quantum Yields for CO_2 Uptake in C-3 and C-4 Plants: Dependence on Temperature, CO_2, and O_2 Concentration. *Plant Physiol.* **1977**, *59*, 86−90.

(10) Kievit, O.; Brudvig, G. W. Direct Electrochemistry of Photosystem I. *J. Electroanal. Chem.* **2001**, *497*, 139−149.

(11) Muller, M. G.; Niklas, J.; Lubitz, W.; Holzwarth, A. R. Ultrafast Transient Absorption Studies on Photosystem I Reaction Centers from Chlamydomonas Reinhardtii. 1. A New Interpretation of the Energy Trapping and Early Electron Transfer Steps in Photosystem I. *Biophys. J.* **2003**, *85*, 3899−3922.

(12) Grotjohann, I.; Fromme, P. Structure of Cyanobacterial Photosystem I. *Photosynth. Res.* **2005**, *85*, 51−72.

(13) Karapetyan, N. V. Interaction of Pigment-Protein Complexes Within Aggregates Stimulates Dissipation of Excess Energy. *Biochemistry* **2004**, *69*, 1299−1304.

(14) Karapetyan, N. V.; Shubin, V. V.; Strasser, R. J. Energy Exchange Between the Chlorophyll Antennae of Monomeric Subunits Within the Photosystem I Trimeric Complex of the Cyanobacterium Spirulina. *Photosynth. Res.* **1999**, *61*, 291−301.

(15) Ciesielski, P. N.; Faulkner, C. J.; Irwin, M. T.; Gregory, J. M.; Tolk, N. H.; Cliffel, D. E.; Jennings, G. K. Enhanced Photocurrent Production by Photosystem I Multilayer Assemblies. *Adv. Funct. Mater.* **2010**, *20*, 4048−4054.

(16) Amunts, A.; Drory, O.; Nelson, N. The Structure of a Plant Photosystem I Supercomplex at 3.4 Å Resolution. *Nature* **2007**, *447*, 58−63.

(17) Haehnel, W.; Jansen, T.; Gause, K.; Klosgen, R. B.; Stahl, B.; Michl, D.; Huvermann, B.; Karas, M.; Herrmann, R. G. Electron-Transfer from Plastocyanin to Photosystem-I. *Embo J.* **1994**, *13*, 1028−1038.

(18) Sommer, F.; Drepper, F.; Hippler, M. The Luminal Helix l of PsaB is Essential for Recognition of Plastocyanin or Cytochrome c(6) and Fast Electron Transfer to Photosystem I in Chlamydomonas Reinhardtii. *J. Biol. Chem.* **2002**, *277*, 6573−6581.

(19) Drepper, F.; Hippler, M.; Nitschke, W.; Haehnel, W. Binding Dynamics and Electron Transfer Between Plastocyanin and Photosystem I. *Biochemistry* **1996**, *35*, 1282−1295.

(20) Badura, A.; Guschin, D.; Kothe, T.; Kopczak, M. J.; Schuhmann, W.; Rogner, M. Photocurrent Generation by Photosystem 1 Integrated in Crosslinked Redox Hydrogels. *Energy Environ. Sci.* **2011**, *4*, 2435−2440.

(21) Badura, A.; Guschin, D.; Esper, B.; Kothe, T.; Neugebauer, S.; Schuhmann, W.; Rögner, M. Photo-Induced Electron Transfer Between Photosystem 2 via Cross-linked Redox Hydrogels. *Electroanalysis* **2008**, *20*, 1043−1047.

(22) Heller, A. Electrical Connection of Enzyme Redox Centers to Electrodes. *J. Phys. Chem.* **1992**, *96*, 3579−3587.

(23) Badura, A.; Kothe, T.; Schuhmann, W.; Rogner, M. Wiring Photosynthetic Enzymes to Electrodes. *Energy Environ. Sci.* **2011**, *4*, 3263−3274.

(24) Utschig, L. M.; Dimitrijevic, N. M.; Poluektov, O. G.; Chemerisov, S. D.; Mulfort, K. L.; Tiede, D. M. Photocatalytic Hydrogen Production from Noncovalent Biohybrid Photosystem I/Pt Nanoparticle Complexes. *J. Phys. Chem. Lett.* **2011**, *2*, 236−241.

(25) Habermüller, K.; Ramanavicius, A.; Laurinavicius, V.; Schuhmann, W. An Oxygen-Insensitive Reagentless Glucose Biosensor

Based on Osmium-Complex Modified Polypyrrole. *Electroanalysis* **2000**, *12*, 1383−1389.
(26) Weiss, J. N. The Hill Equation Revisited: Uses and Misuses. *FAESB J.* **1997**, *11*, 835−841.
(27) LeBlanc, G.; Chen, G. P.; Gizzie, E. A.; Jennings, G. K.; Cliffel, D. E. Enhanced Photocurrents of Photosystem I Films on p-Doped Silicon. *Adv. Mater.* **2012**, *24*, 5959−5962.
(28) Gregg, B. A.; Heller, A. Redox Polymer-Films Containing Enzymes 0.1. A Redox-Conducting Epoxy Cement - Synthesis, Characterization, and Electrocatalytic Oxidation of Hydroquinone. *J. Phys. Chem.* **1991**, *95*, 5970−5975.
(29) International, A. *ASTM G173 - 03(2012), Standard Tables for Reference Solar Spectral Irradiances: Direct Normal and Hemispherical on 37° Tilted Surface*, 2012.